

GRAVITATIONAL WAVE ASTRONOMY —  
AVANT LE DÉLUGE\*

KEITH RILES

for the LIGO Scientific Collaboration, Virgo Collaboration  
and KAGRA Collaboration

University of Michigan, USA

*Received 13 January 2023, accepted 10 March 2023,  
published online 13 June 2023*

The era of gravitational-wave (GW) astronomy is now well under way, with nearly 100 compact binary coalescences (CBCs) confidently detected in the first three observing runs of LIGO and Virgo. With the fourth observing run of LIGO, Virgo, and KAGRA starting in early 2023, it is timely to review what has been learned so far, both from the CBC events and from the absence of other types of GW detections, particularly continuous radiation. Prospects for making such new discoveries soon will be discussed, along with the potential insights to be gained from the deluge of CBC events expected in the coming years and decades.

DOI:10.5506/APhysPolBSupp.16.6-A1

**1. Introduction**

As the fourth observing run (O4) of the LIGO Scientific Collaboration, Virgo Collaboration, and KAGRA Collaboration (LVK) approaches, this article summarizes briefly what has been learned from gravitational wave detections and non-detections to date. All of the detections ( $\sim 90$ ) have come from compact binary coalescences (CBCs): binary black hole (BBH), neutron star (BNS), or neutron star/black hole (NSBH) systems. There have been no detections yet from supernovae or other non-CBC transients, from stochastic radiation (cosmological or astrophysical), or from continuous-wave (CW) sources. Below, we summarize the CBC detections and CW non-detections, concluding with a discussion of future prospects.

To date, there have been three observing runs of the advanced detectors [1–3]: O1 — September 12, 2015 to January 12, 2016 (LIGO Hanford detector, LIGO Livingston detector); O2 — November 30, 2016 to August

---

\* Presented at the 8<sup>th</sup> Conference of the Polish Society on Relativity, Warsaw, Poland, 19–23 September, 2022.

25, 2017 (LIGO detectors with the Virgo detector joining August 1, 2017); and O3 — April 1, 2019 to March 27, 2020 (LIGO and Virgo detectors). The amplitude spectral noise densities for the detectors in the different runs are shown in Fig. 1 [4].

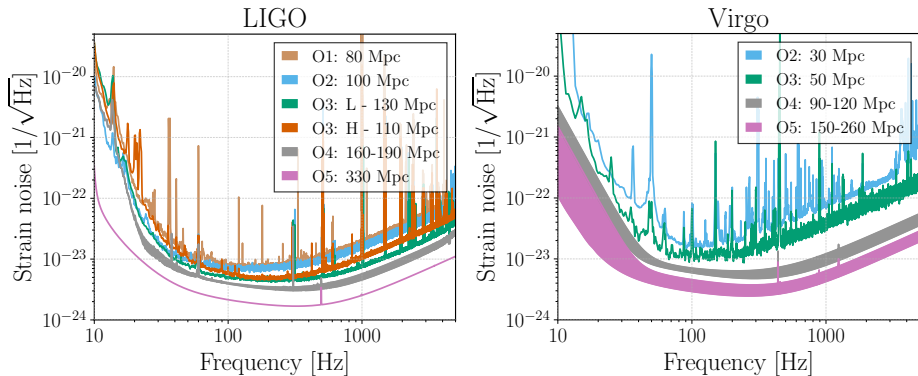


Fig. 1. Strain amplitude spectral noise densities measured for the LIGO and Virgo detectors during the first three observing runs (O1–O3), along with projected sensitivities for the future O4 and O5 runs. The ranges indicate the average distance to which a BNS merger can be detected.

## 2. Compact binary coalescences

Gravitational wave astronomy began dramatically in the O1 run with the discovery of GW150914 [5] on September 14, 2015 (hence the event name), a coalescence of two stellar black holes of primary mass  $m_1 \approx 36 M_\odot$  and secondary mass  $m_2 \approx 29 M_\odot$ , during which approximately  $3 M_\odot$  of gravitational wave energy was released. Figure 2 shows nearly raw detected waveforms, reconstructed waveforms, residuals, and spectrograms from the LIGO Hanford and LIGO Livingston detectors. The close agreement between detected and reconstructed waveforms based on Einstein’s General Theory of Relativity was a stunning confirmation of the theory in a dynamic and strong regime of gravity, as was the excellent agreement between system parameters inferred from the inspiral phase and from the merger phase.

An additional nine BBH mergers were observed collectively in the O1 run and in the longer, more sensitive O2 run, but most exciting was the first detection of a BNS merger (GW170817, see Fig. 2 for spectrograms) [6]. A campaign by 70 different observational teams using ground-based and satellite instruments to identify electromagnetic counterpart radiation was remarkably successful. Signals were detected in gamma-ray, X-ray, ultraviolet, visible, infrared, and radio bands of radiation, confirming the associ-

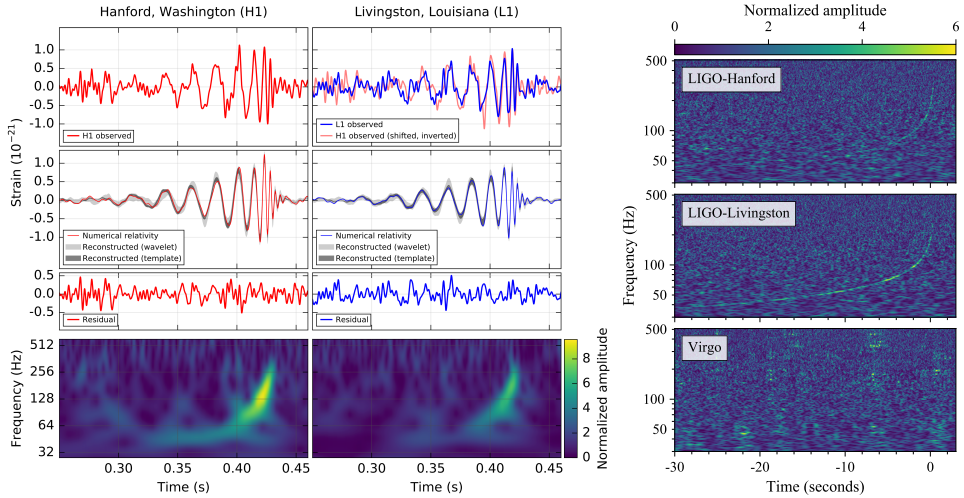


Fig. 2. Left panel — GW150914 (BBH): Top row: detected waveforms in the LIGO Hanford and Livingston detectors; second row: reconstructed waveforms compatible with General Relativity; third row: residuals; fourth row: spectrograms. Right panel — GW170817 (BNS): Spectrograms from the LIGO and Virgo detectors.

ation of short gamma-ray bursts with BNS mergers. The observations also confirmed the “kilonova” hypothesis that the excess neutron material not immediately swallowed in the merger leads to production of heavy elements, such as gold and uranium [7]. Key to the electromagnetic follow-up by telescopes was the sky localization from timing triangulation and from antenna pattern favorability. Although the Virgo GW170817 spectrogram in Fig. 2 shows no evidence of a signal, that very absence was critical to inferring that the source lay very near a Virgo antenna pattern node, dramatically reducing the source location uncertainty [7].

The significant improvement in detector sensitivity achieved for the O3 run led to an increased event rate and a more diverse sample of CBC mergers. Especially notable events included GW190425 (second detected BNS) [8], GW190814 (BBH or possibly NSBH) [9] with large mass asymmetry  $m_1 \gg m_2$  and secondary mass value  $m_2$  lying just above the expected maximum value for neutron stars. Another exceptional event was GW190521 (BBH) [10], which had both a primary and secondary mass near or in an expected high-mass gap due to pulsational pair instability. When the initial two massive BHs merged, they formed a final BH well above  $100 M_\odot$ , making this event the first detection of an intermediate-mass black hole. The waveforms and spectrograms observed for this event in the three detectors are shown in Fig. 3.

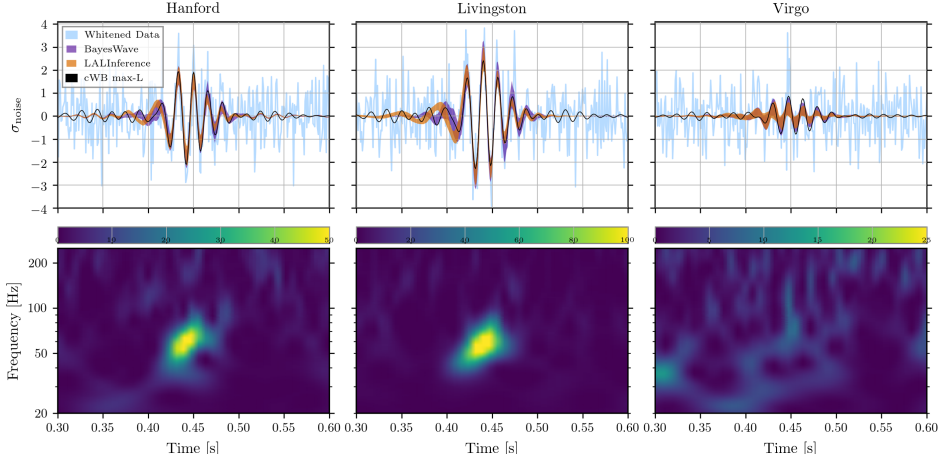


Fig. 3. Waveforms and spectrograms for GW190521 in which two very massive black holes merged to form an intermediate mass black hole. The short duration and low final frequency of the merger characterize massive mergers.

By the end of the O3 run, a total of 90 CBC events had been detected with confidence [11] over the three runs to date. Figure 4 shows the posterior distributions for individual chirp mass ( $\mathcal{M} \equiv (m_1 m_2)^{3/5} / (m_1 + m_2)^{1/5}$ ) governing frequency evolution for the BBH mergers. Also shown is an inferred chirp mass population distribution, corrected for selection effects, most no-

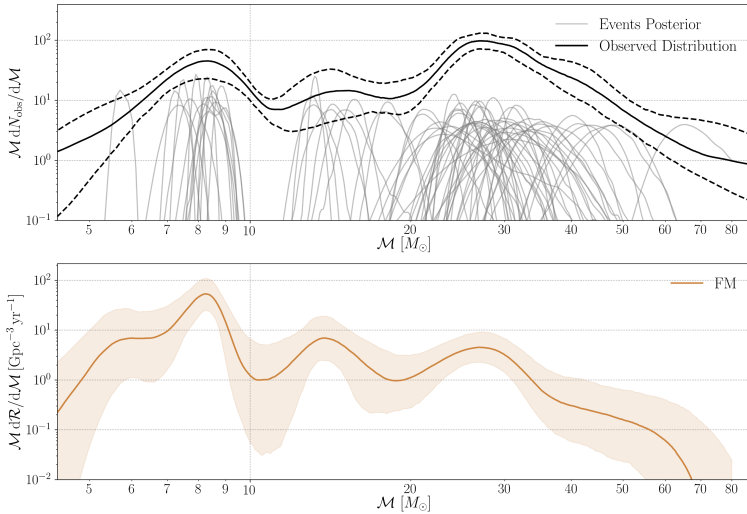


Fig. 4. Top panel: Posterior distributions of chirp masses for individual BBH events observed in the observing runs O1–O3. Bottom panel: Inferred population distribution of merger chirp mass corrected for selection effects.



tably that favoring heavy systems, which can be seen to larger distances [12]. The population distribution shows strong evidence for structure, suggesting more than one channel of BBH formation and perhaps suggesting a contribution from successive, hierarchical BBH mergers [12].

### 3. Continuous wave sources

To date, only upper limits have been obtained in a multitude of searches for continuous gravitational waves [13], for which only a small sample are summarized here. The most sensitive searches are those for known pulsars for which electromagnetic astronomers provide timing ephemerides. Under the nominal assumption that gravitational radiation has twice the frequency of rotation, one can define an optimal search filter in a *targeted* search. For other sources, such as central compact objects (CCOs) at the centers of supernova remnants from which no pulsations have been detected, or low-mass X-ray binary systems, such as Scorpius X-1, one must use *directed* search techniques, which are necessarily less sensitive (by an order of magnitude or more) because of the large statistical trials factor from searching over frequency and phase parameters. Searches with still larger statistical trials factors are *all-sky* surveys for isolated or binary CW sources.

Figure 5 shows (left panel) 95% C.L. upper limits from targeted searches for 236 known pulsars [14], for which the best strain upper limits reach as low as  $\sim 5 \times 10^{-27}$ . One useful benchmark for known pulsars is the indirect upper limit on strain found from assuming that all of the rotational kinetic

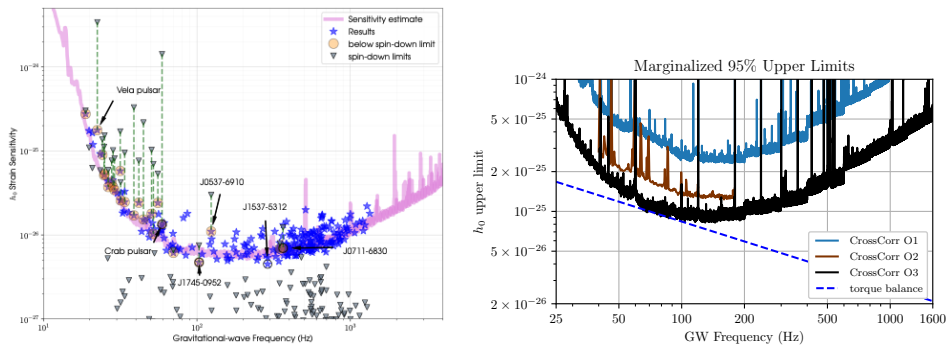


Fig. 5. Left panel: Upper limits (95% C.L.) on GW strain amplitudes for 236 known pulsars. Also shown are corresponding indirect upper limits based on energy conservation. Right panel: Upper limits (95% C.L.) on GW strain amplitude *vs.* frequency for different search methods for Scorpius X-1, shown with the expectation from torque balance for a range of assumed inclination angles, including the value favored by radio observations.

energy loss inferred from frequency spin-down is due to gravitational wave energy emission. Figure 5 shows these benchmark strains for the pulsars, 23 of which are higher than the direct upper limits obtained in the searches.

The right panel of Fig. 5 shows strain upper limits from directed searches for Scorpius X-1, which reach only as low as  $\sim 10^{-25}$  [15], since the spin frequency of the star is unknown, and some orbital parameters have substantial uncertainties. For this low-mass X-ray binary system undergoing accretion, a useful benchmark comes from equating the angular momentum lost to gravitational wave emission to that gained from accretion, leading to a torque balance strain limit *vs.* frequency, also shown in the figure under conservative assumptions.

Figure 6 shows upper limits for the CCOs Cassiopeia A and Vela Jr. from directed searches [16] which reach a bit lower ( $\sim 6 \times 10^{-26}$ ) than for Scorpius X-1, since there are no orbital parameters over which to search. For supernova remnants of known age and distance, another (frequency-independent) benchmark can be defined without knowing the rotational frequency by assuming that during the lifetime of the star, its rotational kinetic energy loss has been dominated by gravitational wave energy emission. Figure 6 includes these benchmarks as horizontal lines (solid for Cassiopeia A; dashed and dotted for two different assumed ages/distances for Vela Jr.).

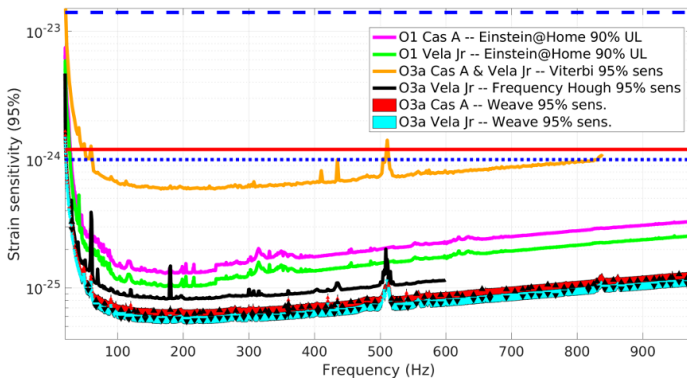


Fig. 6. Upper limits (95% C.L.) on GW strain amplitude *vs.* frequency for the supernova remnant central compact objects Cassiopeia A and Vela Jr. from several search methods and data runs.

Figure 7 shows 95% C.L. upper limits from all-sky searches for unknown isolated stars [17], which reach only as low as  $\sim 10^{-25}$ , thanks to large trials factors.

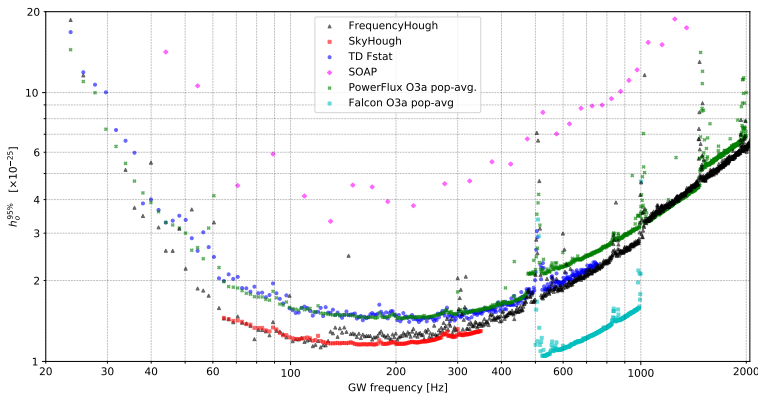


Fig. 7. Upper limits (95% C.L.) on GW strain amplitudes *vs.* frequency for several all-sky searches for isolated stars.

#### 4. Outlook

Event rates for the upcoming O4 run are expected to be significantly higher than for O3, and the rates for the O5 run are expected to be still higher, as additional detector upgrades are implemented in the LIGO and Virgo detectors. The KAGRA detector will be also improving its sensitivity and may soon begin to contribute additional detections and sky localization information. One can expect hundreds, if not more, of detected CBC events in the coming years, ideally with one or more detected electromagnetic counterparts. Looking farther ahead, there will likely be still more upgrades of the LIGO and Virgo detectors beyond O5. Farther out there is the prospect of “3<sup>rd</sup>-generation” detectors: Einstein Telescope [18] and Cosmic Explorer [19]. At their design sensitivities, they would be able to detect a significant fraction of all CBC mergers in the visible universe. In fact, they should be able to detect mergers — if they occurred — from a time before the first stars were formed, due to primordial black holes.

The outlook for the first detection of continuous gravitational waves is uncertain [13]. That first discovery could come this year, or not for a decade or more. Theoretical uncertainties on expected non-axisymmetries are too large for confident prediction, but when those first detections are made they will likely provide sources, unlike the individual CBC mergers, that can be followed and studied with ever greater precision, for generations to come.

Acknowledgements in <https://dcc.ligo.org/LIGO-P2100218/public>

## REFERENCES

- [1] LIGO Scientific Collaboration (J. Aasi *et al.*), *Class. Quantum Grav.* **32**, 074001 (2015).
- [2] F. Acernese *et al.*, *Class. Quantum Grav.* **32**, 024001 (2015).
- [3] T. Akutsu *et al.*, *Prog. Theor. Exp. Phys.* **2021**, 05A102 (2021).
- [4] KAGRA Collaboration, LIGO Scientific Collaboration, Virgo Collaboration (B.P. Abbott *et al.*), *Living Rev. Relativ.* **23**, 3 (2020).
- [5] LIGO Scientific Collaboration, Virgo Collaboration (B.P. Abbott *et al.*), *Phys. Rev. Lett.* **116**, 131103 (2016).
- [6] LIGO Scientific Collaboration, Virgo Collaboration (B.P. Abbott *et al.*), *Phys. Rev. Lett.* **119**, 161101 (2017).
- [7] B.P. Abbott *et al.*, *Astrophys. J. Lett.* **848**, L12 (2017).
- [8] B.P. Abbott *et al.*, *Astrophys. J. Lett.* **892**, L3 (2020).
- [9] R. Abbott *et al.*, *Astrophys. J. Lett.* **896**, L44 (2020).
- [10] LIGO Scientific Collaboration, Virgo Collaboration (R. Abbott *et al.*), *Phys. Rev. Lett.* **125**, 101102 (2020).
- [11] LIGO Scientific Collaboration, Virgo Collaboration, KAGRA Collaboration (R. Abbott *et al.*), [arXiv:2111.03606 \[gr-qc\]](#).
- [12] LIGO Scientific Collaboration, Virgo Collaboration, KAGRA Collaboration (R. Abbott *et al.*), *Phys. Rev. X* **13**, 011048 (2023), [arXiv:2111.03634 \[astro-ph.HE\]](#).
- [13] K. Riles, *Living Rev. Relativ.* **26**, 3 (2023), [arXiv:2206.06447 \[astro-ph.HE\]](#).
- [14] R. Abbott *et al.*, *Astrophys. J.* **935**, 1 (2022).
- [15] R. Abbott *et al.*, *Astrophys. J. Lett.* **941**, L30 (2022).
- [16] LIGO Scientific Collaboration, Virgo Collaboration (R. Abbott *et al.*), *Phys. Rev. D* **105**, 082005 (2022).
- [17] LIGO Scientific Collaboration, Virgo Collaboration, KAGRA Collaboration (R. Abbott *et al.*), *Phys. Rev. D* **106**, 102008 (2022).
- [18] M. Punturo *et al.*, *Class. Quantum Grav.* **27**, 084007 (2010).
- [19] M. Evans *et al.*, «A Horizon Study for Cosmic Explorer Science, Observatories, and Community», Tech. Rep. CE-P2100003-v7, October 2021 (<https://cosmicexplorer.org/dcc.html>).